Cellular mechanical properties reflect the differentiation potential of adipose-derived mesenchymal stem cells

Rafael D. González-Cruz[a,b,1], Vera C. Fonseca[a,b,1], and Eric M. Darling[a,b,c,d,2]

[a]Department of Molecular Pharmacology, Physiology, and Biotechnology; [b]Center for Biomedical Engineering; [c]Department of Orthopaedics; and [d]School of Engineering, Brown University, Providence, RI 02912

Edited by David A. Weitz, Harvard University, Cambridge, MA, and approved April 12, 2012 (received for review December 9, 2011)

The mechanical properties of adipose-derived stem cell (ASC) clones correlate with their ability to produce tissue-specific metabolites, a finding that has dramatic implications for cell-based regenerative therapies. Autologous ASCs are an attractive cell source due to their immunogenicity and multipotent characteristics. However, for practical applications ASCs must first be purified from other cell types, a critical step which has proven difficult using surface-marker approaches. Alternative enrichment strategies identifying broad categories of tissue-specific cells are necessary for translational applications. One possibility developed in our lab uses single-cell mechanical properties as predictive biomarkers of ASC clonal differentiation capability. Elastic and viscoelastic properties of undifferentiated ASCs were tested via atomic force microscopy and correlated with lineage-specific metabolite production. Cell sorting simulations based on these "mechanical biomarkers" indicated they were predictive of differentiation capability and could be used to enrich for tissue-specific cells, which if implemented could dramatically improve the quality of regenerated tissues.

cell mechanics | mesenchymal stem cell enrichment | viscoelasticity | single-cell characterization | AFM

Adipose tissue contains a heterogeneous population of mesenchymal stem cells (MSCs) known as adipose-derived stem cells (ASCs) (1). ASCs are capable of differentiating into a variety of lineage-specific cell types, including adipocytes, osteoblasts, and chondrocytes (1–3). In comparison to MSCs derived from other tissues, ASCs are simple to isolate and available in large quantities (4, 5). Because of the cells' mesodermal origin, ASCs have been used for many soft tissue and orthopaedic applications (6–10). Unfortunately, ASC isolation is confounded by the lack of distinct and universally effective MSC biomarkers. Adipose tissue contains multiple cell types, including mature adipocytes, fibroblasts, smooth muscle cells, and endothelial cells (11), which can contaminate the stromal fraction collected during ASC isolation. While conventional methods such as flow cytometry can isolate stem cells using surface antigen expression (1, 2, 12), resulting cell yields are often less than 1% (13, 14). Furthermore, the surface antigens present on ASCs can also be found on other cell types in adipose tissue, complicating the isolation of pure mesenchymal stem cell populations (15–17). Collectively, these limitations suggest a need for alternative biomarkers that allow for ASC enrichment based on lineage potential.

Recently, single-cell mechanical properties were found to be akin to gene and protein expressions, capable of distinguishing differences in cellular subpopulations, disease state, and tissue source (18–22). Cells display varying levels of resistance to deformation (elasticity) and flow (viscosity) in response to an applied force. This behavior depends on the composition and organization of subcellular structures, particularly the cytoskeleton. Previous studies describe the use of atomic force microscopy (AFM) to discriminate between elastic/viscous properties of MSCs and differentiated cells (18–21). From this work, a common set of parameters has been identified that act as mechanical biomarkers suitable for comparing among distinct cell types. These biomarkers describe the deformation response of a cell and include the elastic modulus (E_{elastic}), instantaneous modulus (E_0), relaxed modulus (E_R), apparent viscosity (μ), and cell size/height. These parameters are obtained by modeling the cell as a standard linear solid and acquiring data from indentation and stress relaxation tests (21). In brief, E_{elastic} represents the compliancy of the cell during a simple indentation test, E_0 and E_R are the initial and final moduli, respectively, during a stress relaxation test, and the apparent viscosity is a descriptor of how the cell deforms over time (see *SI Text* for more detail). It is hypothesized that ASC mechanical biomarkers can be used to indicate not only cell type but also predict tissue-specific differentiation potential for stem cells.

The goal of this study was to investigate the relationship between the mechanical properties of ASCs and their lineage differentiation capabilities. Specifically, 32 single-cell-derived clonal populations were established using ASCs harvested from human, subcutaneous fat. Cellular elastic and viscoelastic properties for each clonal population were determined via AFM by testing individual cells. Clones were then assessed for differentiation potential along adipogenic, osteogenic, and chondrogenic lineages. Correlations were determined between individual mechanical parameters and metabolite production, and simulations were used to determine potential tissue-specific enrichment for mechanical property-based sorting approaches.

Results

Single-cell mechanical properties were measured using AFM for 32 ASC clonal populations. Cells were assessed in both spherical and spread morphologies by testing samples soon after seeding (approximately 30 min) or after one day. For both morphologies, cells were firmly attached to the underlying glass substrate during testing (Fig. S1). Clones exhibited substantial heterogeneity in their mean elastic and viscoelastic properties (Fig. 1; Fig. S2). When compared to spread ASCs, spherical cells were significantly more compliant, taller, and less viscous (Table 1). These expected results are associated with differences in cytoskeletal organization between spherical and spread morphologies. Regardless of cell shape, elastic and viscoelastic data fit well to Hertzian-based mathematical models ($R^2_{\text{elastic}} = 0.99$, $R^2_{\text{viscoelastic}} = 0.87$).

All ASC clonal populations were assessed for multipotentiality by differentiation along the adipogenic, osteogenic, and chondro-

Author contributions: E.M.D. designed research; R.D.G.-C., V.C.F., and E.M.D. performed research; R.D.G.-C. and E.M.D. analyzed data; and R.D.G.-C. and E.M.D. wrote the paper.

The authors declare no conflict of interest.

This article is a PNAS Direct Submission.

[1]R.D.G.-C. and V.C.F. contributed equally to this work.

[2]To whom correspondence should be addressed. E-mail: Eric_Darling@brown.edu.

See Author Summary on page 9234 (volume 109, number 24).

This article contains supporting information online at www.pnas.org/lookup/suppl/doi:10.1073/pnas.1120349109/-/DCSupplemental.

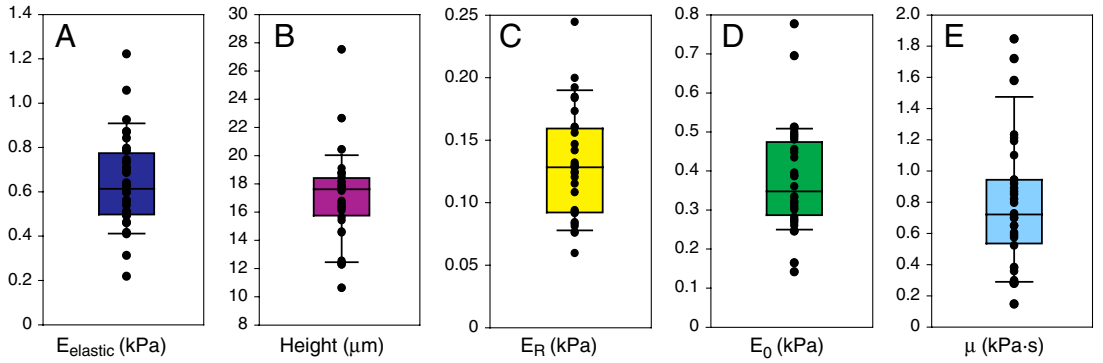

Fig. 1. The mechanical properties of ASCs were heterogeneous, a finding that was examined as a possible means to identify lineage-specific subpopulations. Elastic and viscoelastic properties of 32 ASC clones with spherical morphologies were measured via AFM indentation and stress relaxation tests, respectively. Within each clonal population, an average of 22 cells was tested. The following cellular mechanical properties were measured: elastic modulus (*A*), cell height (*B*), relaxed modulus (*C*), instantaneous modulus (*D*), and apparent viscosity (*E*). Elastic and viscoelastic data fit well to Hertzian mathematical models ($R^2 = 0.99$ and $R^2 = 0.87$, respectively). Data are presented as box-whisker plots overlaid with the individual geometric means of each clone.

genic lineages (Fig. 2). Standard biochemical assays were used to quantify lineage-specific metabolite production on a per-cell or per-DNA basis. For each biochemical analysis, clones were arranged in ascendant order of lineage-specific metabolite production (Fig. 3). Positive differentiation was noted for samples that exhibited metabolite production above the 90th percentile of corresponding controls cultured in noninduction medium. Overall, 44% of clones were tripotent, 47% were bipotent, and 9% were unipotent. No clones showed a total lack of differentiation capability.

For each lineage, significant differences in metabolite production existed between differentiated and undifferentiated ASCs. Oil Red O optical densities for clones in adipogenic conditions were significantly greater than those of undifferentiated controls ($P < 0.001$). Of all clones tested, 69% exhibited positive adipogenic differentiation. Alizarin Red S optical densities for clones in osteogenic conditions were also significantly greater than those of undifferentiated controls ($P < 0.001$). Of all clones tested, 75% exhibited osteogenic differentiation potential. Lastly, sulfated glycosaminoglycan (sGAG) deposition for clones in chondrogenic conditions was significantly greater than those of undifferentiated controls ($P < 0.001$). Positive chondrogenic differentiation was observed for 91% of all clones. In addition, immunostaining revealed robust synthesis of type II collagen for induced groups but not undifferentiated controls.

The hypothesis that cellular mechanical biomarkers can be used as predictors of ASC differentiation potential was examined by determining correlations between ASC mechanical properties and lineage-specific metabolite production. Significant correlations existed for spherical cellular mechanical properties and the three lineages examined (Table 2; Fig. S3), supporting the stated hypothesis and suggesting a novel means of classifying undifferentiated ASCs into tissue-specific groups. Analyses showed that adipogenesis was positively correlated with cell height and negatively correlated with $E_{elastic}$, E_R, and E_0. Osteogenesis was positively correlated with $E_{elastic}$, E_R, and E_0. Chondrogenesis was positively correlated with $E_{elastic}$ and μ. The relative magnitude of the relationships was assessed by comparing slopes calculated from linear fits of normalized metabolite production per mechanical parameter. Generally, the osteogenic lineage was associated with steeper, positive slopes, followed by the chondrogenic lineage with shallower, positive slopes, and the adipogenic lineage with negative slopes. This relationship was reversed with respect to cell height. Surprisingly, no significant correlations were found using the mechanical properties of spread ASCs (Table S1). This finding might be expected based on previous reports that stem cells exhibit consistent mechanical properties

Table 1. Summary of cellular mechanical properties for ASC clonal populations

Morphology	$E_{elastic}$ (kPa)	E_0(kPa)	E_R(kPa)	μ (kPa·s)	Height (μm)
Spherical	0.6 ± 0.2	0.4 ± 0.1	0.1 ± 0.04	0.7 ± 0.4	16.9 ± 3.1
Spread	1.6 ± 0.5	1.1 ± 0.3	0.6 ± 0.2	2.6 ± 1.6	4.6 ± 0.5

Cellular mechanical properties are indicated by the following abbreviations: $E_{elastic}$ (elastic modulus), E_{equil} (equilibrium modulus), E_0 (instantaneous modulus), E_R (relaxed modulus), μ (apparent viscosity), and *Height* (cell height). Tabular data is presented as geometric means ± SD. Student's *t*-tests between spherical and spread ASCs demonstrated significant differences between morphologies for all comparisons ($P < 0.001$).

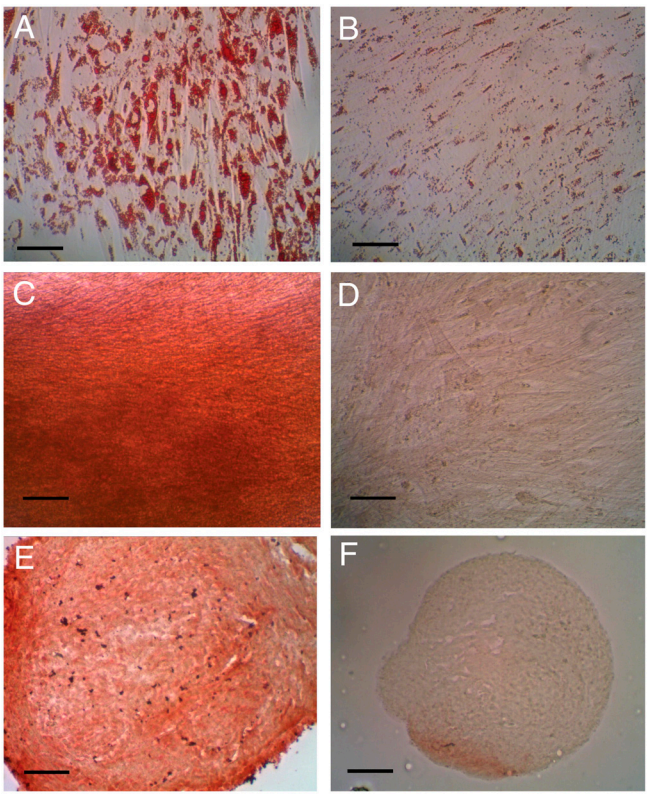

Fig. 2. ASC differentiation toward mesodermal lineages was confirmed via lineage-specific metabolite detection assays. Adipogenic differentiation was assessed by Oil Red O staining of intracellular lipid production in induced (*A*) and control (*B*) samples. Osteogenic differentiation was assessed by Alizarin Red S staining of calcified matrix in induced (*C*) and control (*D*) samples. Chondrogenic differentiation was assessed by type II collagen immunostaining in induced (*E*) and control (*F*) samples. (Scale bars, 100 μm).

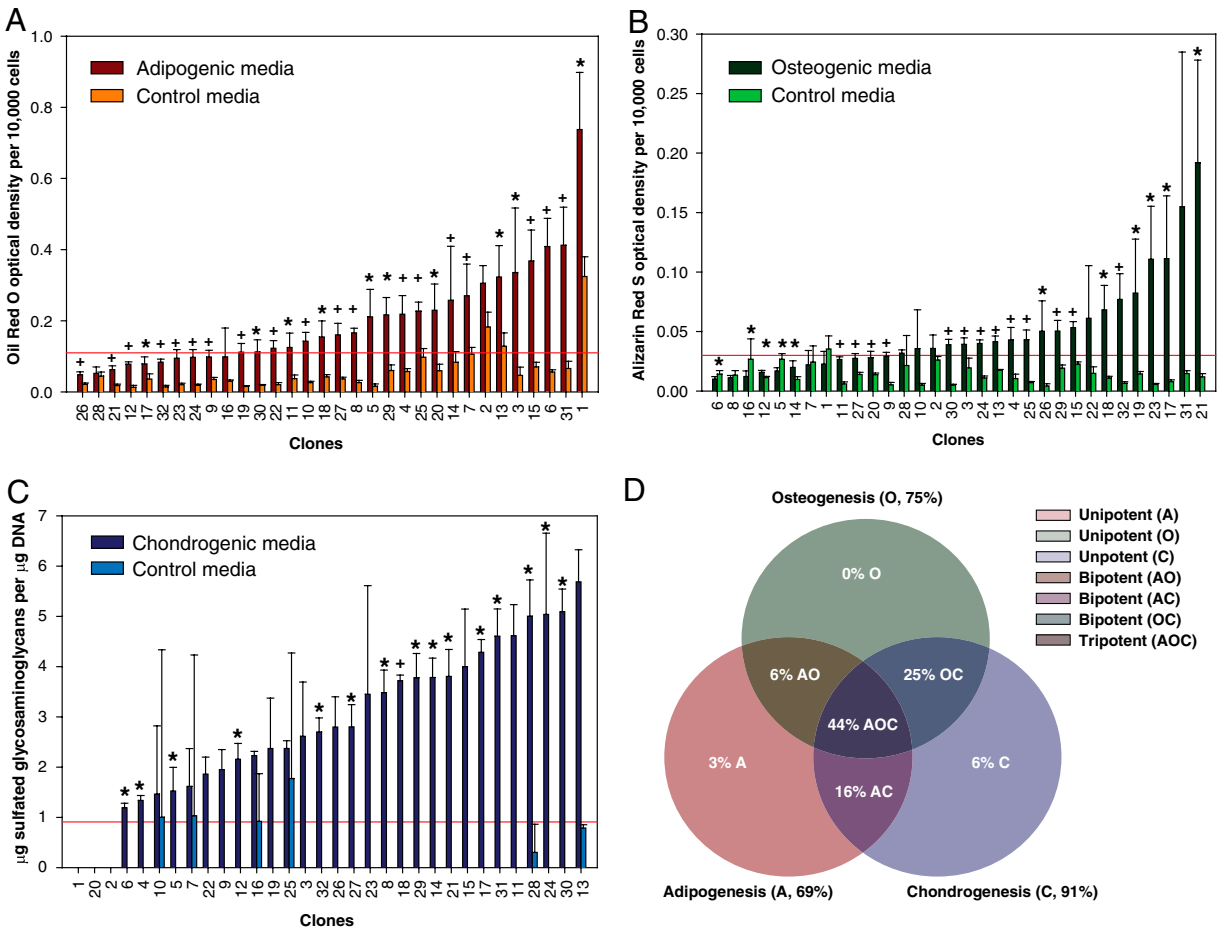

Fig. 3. Amounts of lineage-specific metabolites were determined by clone for adipogenesis (*A*), osteogenesis (*B*), and chondrogenesis (*C*). Each differentiation lineage showed extensive variability in metabolite production, emphasizing heterogeneity among the clonal populations. For each graph, the red line represents the 90th percentile associated with undifferentiated controls. This level acted a threshold value indicating positive or negative differentiation. Results were used to determine the multipotentiality of clones investigated in this study (*D*). Data are presented as arithmetic means ± SD. Single asterisks denote statistical significance at $\alpha = 0.05$, whereas plus signs denote statistical significance at $\alpha = 0.001$ from corresponding controls.

when firmly attached compared to the suspended state (23). Additionally, no discernible relationship existed between the mechanical properties of clones and uni/bi/tri-lineage potency states (Table S2; Fig. S4).

According to the current findings, these mechanical biomarkers could be used to sort ASCs into mechanically similar groups that correspond to specific lineages. Although lineage-specific metabolite production varied among clones, a subset could be considered high-potential populations. These groups of clones were defined as the top quartile of all populations examined, based on lineage-specific metabolite production, and are proposed as highly desirable, ASC subpopulations. The mechanical biomarkers for these clones showed distinct differences from the other populations (Fig. 4*A*). Highly osteogenic clones exhibited significantly higher E_{elastic}, E_R, and E_0 values ($P < 0.05$, $P < 0.001$, and $P < 0.01$, respectively). Highly chondrogenic clones showed significantly higher μ values ($P < 0.05$). While not statistically significant, highly adipogenic clones were generally larger ($P = 0.09$) and more compliant ($P = 0.11$) than other clones.

Sorting simulations based on these mechanical parameters demonstrated the degree of lineage-specific enrichment possible using only cellular mechanical properties (Fig. 4*B*). Threshold values were determined for adipogenesis, osteogenesis, and chondrogenesis by assessing the effect of cell height, E_R, and μ, respectively, on population descriptors such as lineage-capable purity, high potential purity, and overall cell yield (Fig. 4 *C*–*E*). Results showed that as progressively stricter sorting parameters were used, lineage-specific clone purity increased while cell yield decreased. High-potential populations typically were the larger (adipogenesis), stiffer (osteogenesis), or more viscous (chondrogenesis) clones, and therefore could be enriched simply by raising the corresponding threshold sorting parameters. For example, if only clones greater than 20 μm in cell height were collected, purity of adipogenic-positive clones was increased by 45%. Furthermore, the purity of highly adipogenic clones increased by 170%. Osteogenic clones could be enriched by selecting cells with $E_R > 0.2$ kPa, which resulted in a 33% increase in osteogenic-positive clones and a 300% increase in highly osteogenic clones. Chondrogenic clones could be selected using $\mu > 1.6$ kPa·s, resulting in a 10% increase in chondrogenic-positive cells and a 300% increase in highly chondrogenic clones. Total cell yield for these three cases would be 9%, 3%, and 6%, respectively, a substantial improvement over many antigen-based sorting schemes that result in <1% yields.

Discussion

The results of this study indicate that cellular mechanical properties are predictive of ASC differentiation and synthetic potential. Significant correlations existed between mechanical properties and lineage-specific metabolite production by ASC clones. These findings represent an advantageous means to characterize the differentiation potential of stem cells. Surface antigen-based enrichment techniques have had limited success identifying a stem cell biomarker useful for sorting ASCs (24). High specificity is an

Table 2. Correlations between ASC mechanical properties and their differentiation potential

Mechanical property (MP)	Lineage	Pearson's r (±95% CI)	*P*-value	Normalized metabolite production/ MP × 10^{-3}
$E_{elastic}$	Adipogenic	−0.51 ± 0.27	*0.003*	−1.14
	Osteogenic	0.46 ± 0.28	*0.007*	1.66
	Chondrogenic	0.59 ± 0.24	*0.004*	0.71
E_0	Adipogenic	−0.50 ± 0.27	*0.003*	−1.57
	Osteogenic	0.54 ± 0.26	*0.001*	3.33
	Chondrogenic	0.60 ± 0.23	*0.0003*	1.09
E_R	Adipogenic	−0.49 ± 0.27	*0.005*	−5.54
	Osteogenic	0.48 ± 0.28	*0.005*	10.44
	Chondrogenic	0.31 ± 0.32	0.08	0.26
μ	Adipogenic	−0.27 ± 0.33	0.14	−0.36
	Osteogenic	0.25 ± 0.33	0.16	0.28
	Chondrogenic	0.56 ± 0.25	*0.0008*	0.57
Height	Adipogenic	0.41 ± 0.30	*0.02*	104.37
	Osteogenic	0.04 ± 0.35	0.83	−8.05
	Chondrogenic	0.07 ± 0.35	0.72	18.12

Cellular mechanical properties are indicated by the following abbreviations: $E_{elastic}$ (elastic modulus), E_0 (instantaneous modulus), E_R (relaxed modulus), μ (apparent viscosity), and *Height* (cell height). Error values for Pearson's correlation coefficient *r* represent 95% confidence intervals (95% CI). Correlations were calculated using log-transformed geometric means. To allow for comparisons among lineages, metabolite data were normalized to their respective, lineage-specific arithmetic mean and then fit with a linear regression. The slopes of these fits represent lineage-specific metabolite production per mechanical property (MP) measured as specified by the lineage. Adipogenic, osteogenic, and chondrogenic characteristic metabolites are intracellular lipids, extracellular matrix-bound calcium, and sulfated GAGs, respectively. The mechanical property relationship to osteogenic potential showed steep, positive slopes (stiffer = more osteogenic), whereas adipogenic potential showed negative slopes (more compliant = adipogenic).

advantage for many applications but is nonideal for targeting ASC subpopulations exhibiting variable phenotypes (e.g., multipotency, bipotency, or unipotency). Mechanical properties act as an indicator of the biochemical and structural characteristics of a cell and hold promise as a composite biomarker capable of identifying beneficial ASC subpopulations.

The observed heterogeneity in mechanical properties across clones and between morphologies can be attributed to variations in intracellular composition and organization. Previously, it was shown that differentiated cells and stem cells differ in their elastic and viscoelastic properties (18). As stem cells differentiate toward specific lineages, their cytoskeleton rearranges until differentiation is achieved (25–28). During this process, rearrangement is concurrent with a modulation of the cellular mechanical properties and any accumulation of intracellular metabolites (27). For osteogenesis, cells typically become stiffer, whereas for adipogenesis, cells become more compliant. Chondrogenesis induces intracellular changes that result in higher instantaneous and relaxed moduli as well as higher apparent viscosities (28). These physical changes can occur to varying degrees before irreversible commitment to a single lineage. However, it is hypothesized that an ASC exhibits a mechanical phenotype associated with its preferred lineage, possibly because it has already begun the differentiation process (26). This possibility is not an impediment to practical application, though, because the purpose of tissue-specific enrichment is to collect all cells capable of expressing the proper phenotype whether they are initially multipotent, unipotent, or fully differentiated.

ASC differentiation potentials showed that all clonal populations could differentiate along at least one lineage, while 91% of all clones could successfully differentiate along at least two lineages. Previous ASC clonal studies reported differentiation efficiencies well below the ones found here (1–3). However, differences in isolation and expansion approaches could account for this variation. The current study used the limiting dilution technique to establish single-cell clones, and only clones capable of doubling 20–25 times were evaluated. Furthermore, initial ASCs had already been passaged twice, whereas previous studies typically began with freshly isolated cells. This period of in vitro expansion could bias the cells slightly toward a more differentiation-prone state. Also, freshly isolated ASCs can be contaminated with other cell types present in adipose tissue. The presence of these contaminating cells can affect ASC differentiation potential (29, 30). For example, if fibroblasts make up a significant portion of the harvest population, then overall osteogenic potential could be significantly reduced. Extended culture of undifferentiated ASCs can also affect ultimate differentiation potential. Specifically, monolayer expansion, under the conditions used in the current study, was previously shown to increase the chondrogenic potential of ASCs prior to differentiation (31, 32). Therefore, environmental conditioning could have been influential in the noticeably higher percentage of chondrogenic-positive clones found in this study.

As has been reported previously, adipose tissue contains ASC subpopulations with distinct differentiation potentials (12, 15, 33–35). Surface antigen expression has been used to detect subpopulations capable of lineage-specific differentiation. However, this technique produces low cell yields and requires antibody conjugation, which may affect cellular function (36). There are also concerns regarding ASC purity in these subpopulations because other cells, such as endothelial cells and fibroblasts, are found in the stromal fraction of adipose tissue and share surface antigens with ASCs (15, 34). However, their mechanical properties are distinct from those measured for stem cells (18, 37). Another level of complexity arises when discriminating between cells exhibiting the same surface markers but at different expression levels. The importance of this variation has yet to be investigated. In contrast to these surface antigen approaches, mechanical biomarkers function as a broad indicator of differentiation potential and require no modification of or invasion into individual cells.

Limitations do exist to using mechanical biomarkers for stem cell sorting approaches. Most of these arise from the challenge inherent in rapidly evaluating large cell numbers, which currently is a major advantage of flow cytometery. While AFM is an established technique for accurately measuring cellular elastic and viscoelastic properties, testing the mechanical characteristics of a clinically relevant quantity of ASCs using this technique would be infeasible. Microfluidics-based approaches like cell deformation cytometry, size and physical characteristic sorting, and optical stretchers represent viable solutions to this limitation because of their high-throughput capabilities (23, 38–47). It should be noted that the properties measured in the current study, which were for cells attached to a substrate, are unlikely to translate directly to cells in a fully suspended state. Previous, matched comparisons of AFM to micropipette aspiration results showed that measured modulus values were similar but apparent viscosities were much higher for fully suspended cells (21). The current findings will need to be validated for implementation in a given sorting device, but many of the observed mechanical property differences should be apparent regardless of approach. Ultimately, the specific parameters used to identify targeted cell populations are irrelevant. The device needs only to distinguish among the deformation responses of individual cells and then group them accordingly.

The current study uses a small number of clones that are assumed to be representative of a larger, ASC population. If true, the relationship between mechanical properties and lineage-specific differentiation can be exploited to isolate cells capable of

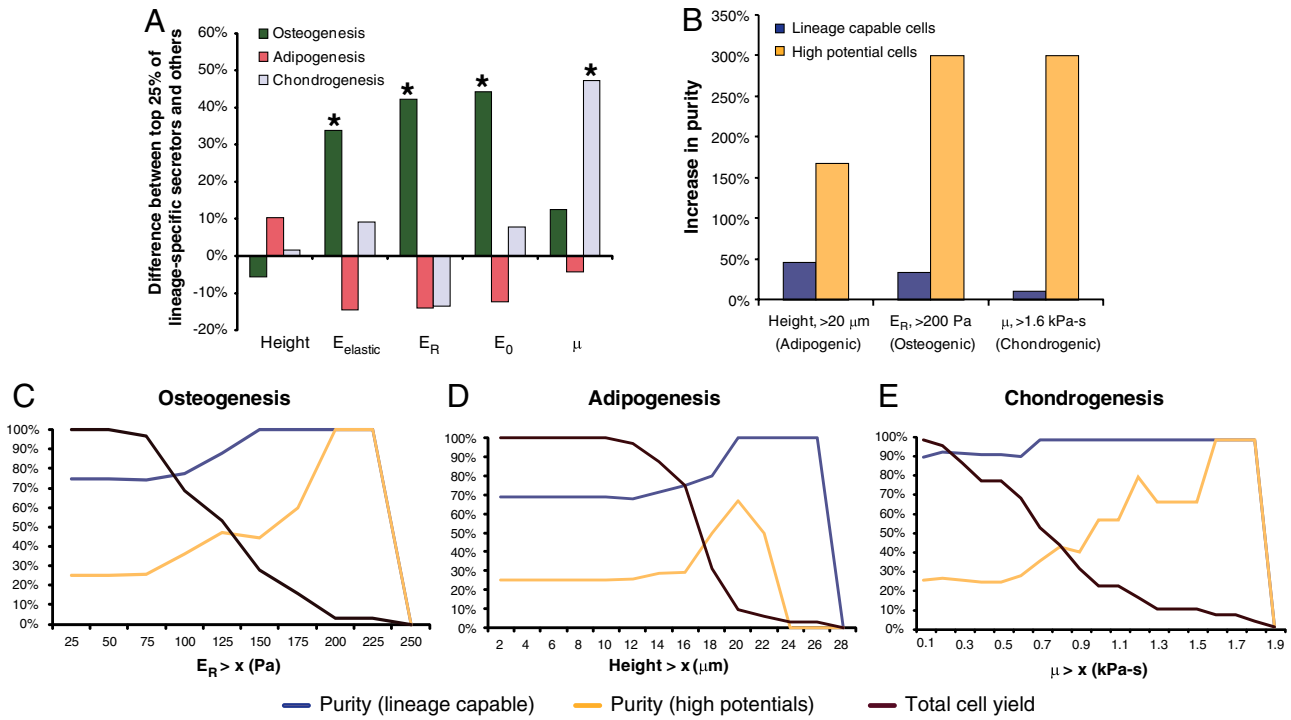

Fig. 4. Mechanical and biochemical data were used to determine whether tissue-specific subpopulations might exist. Clones exhibiting high-differentiation potential for certain lineages exhibited distinct mechanical properties (*A*). Simulations using these predetermined mechanical biomarkers as sorting parameters showed that it would be possible to enrich for ASCs possessing lineage-specific differentiation potentials (*B*). However, higher cell purities were balanced by lower cell yields (*C*–*E*). Single asterisks denote statistical significance at $\alpha = 0.05$ between the upper 25% and lower 75% of clonal populations for each lineage tested.

secreting large amounts of matrix molecules, which are critical for rapid tissue regeneration. The current findings are supported by previous reports of mechanical differences between undifferentiated stem cells and fully differentiated osteoblasts, adipocytes, and chondrocytes (18, 25–27, 48). It remains to be seen whether this mechanical biomarker-lineage relationship can be investigated on a larger scale, as well as whether it will improve functional tissue growth compared to using unsorted populations. Regardless, the results presented here present an intriguing role for the mechanical properties of undifferentiated stem cells. In summary, this study supports the hypothesis that ASC mechanical properties are indicative of differentiation potential. Furthermore, ASCs capable of producing high levels of lineage-specific metabolites were found to be mechanically distinct from other clones and could be a target for cellular enrichment. Simulations using the current data indicated that mechanical biomarker-based sorting would produce significant increases in cell purity. Future studies can build on these findings by targeting mechanically similar subpopulations that are well suited for tissue-specific regeneration.

Materials and Methods

ASC Isolation and Clonal Population Expansion. Primary ASCs (Zen-Bio) were isolated from subcutaneous adipose tissue from healthy, nondiabetic, nonsmoking female donors aged 29–57 y ($N = 7$) and having an average body mass index (BMI) of 27.6 kg/m^2. ASC clonal populations were derived using the limiting dilution cloning method. Passage 2 (P2) ASCs were suspended in conditioned expansion medium (3), diluted to 1 cell/200 μL, and placed into thirty 96-well plates over three sessions. Conditioned expansion medium contained DMEM/F-12 (Lonza), 10% FBS (Zen-Bio), 5 ng/mL epidermal growth factor, 0.25 ng/mL transforming growth factor-beta 1 (TGF-β1), 1 ng/mL basic fibroblastic growth factor (R&D Systems), 100 U/mL penicillin, 100 μg/mL streptomycin, and 0.25 μg/mL amphotericin B, pen/strep/ampB (Invitrogen). Only wells with a single cell were kept to establish true clonal populations. At 90% confluence, clones were transferred to T-75 flasks (P3). At P4, cells were trypsinized, frozen, and kept in liquid nitrogen. Before mechanical and biochemical tests, clones were thawed and passaged once more (to P5).

Adipogenic and Osteogenic Differentiation. ASC clones ($n = 32$) were plated onto 96-well plates at a density of 8,000 cells/well and cultured with expansion medium until confluent. Medium was then replaced with 200 μL of adipogenic induction medium, osteogenic induction medium, or control medium ($n = 6$, 6, and 12, respectively) (3, 49). Adipogenic medium contained DMEM/F-12, 3% FBS, 10 μg/mL insulin, 0.39 μg/mL dexamethasone, 55.6 μg/mL isobutyl-1-methylxanthine (Sigma-Aldrich), 17.5 μg/mL indomethacin (Cayman Chemical), and pen/strep/ampB. Osteogenic medium contained DMEM/F-12, 10% FBS, 2.16 mg/mL β-glycerophosphate (10 mM), 50 μg/mL μascorbate-2-phosphate, 3.92 ng/mL dexamethasone, (Sigma-Aldrich), and pen/strep/ampB. Control medium contained DMEM/F-12, 10% FBS, and pen/strep/ampB. Cells were cultured for three weeks and then fixed in 3.7% paraformaldehyde (EMS). Oil Red O (ORO, Sigma-Aldrich) staining was used to assess lipid accumulation in adipogenic and control samples. Alizarin Red S (ARS, Sigma-Aldrich) staining was used to assess calcified matrix deposition in osteogenic and control samples. After digital images were taken, ORO and ARS dyes were eluted from each sample, and optical densities were measured at 500 nm and 540 nm, respectively (3). At this point, each well was stained with 4′,6-diamino-2-phenylindole (DAPI, Thermo Fisher Scientific), and optical densities were normalized on a per-cell basis (50).

Chondrogenic Differentiation. ASC clones were placed in V-bottomed, 96-well plates at a density of 50,000 cells/well. Plates were centrifuged at 400 g to form cell pellets, and expansion medium was replaced with 200 μL of chondrogenic induction medium ($n = 6$) or control medium ($n = 6$) (3, 49). Chondrogenic medium contained high glucose Dulbecco's Modified Eagle Medium (DMEM), 10% FBS, 10 ng/mL TGF-β1, 50 μg/mL ascorbate-2-phosphate, 39.0 ng/mL dexamethasone, 1% ITS+ Premix (BD Biosciences), and pen/strep/ampB. Cell pellets were maintained in culture for three weeks. For analysis, half of the pellets [chondrogenic ($n = 3$) and control ($n = 3$)] were fixed in 3.7% paraformaldehyde. The remaining pellets were digested with papain (Sigma-Aldrich). Fixed pellets were cryosectioned and immunostained using a Histostain-Plus Kit (Invitrogen) and a primary antibody specific to type II collagen (II-II6B3-s, Developmental Studies Hybridoma Bank). The papain-digested pellets were used to quantify sGAG content via the dimethylmethylene blue assay (Accurate Chem. and Sci. Corp.). The PicoGreen assay (Invitrogen) was used to quantify DNA amounts (480 nm excitation, 520 nm emission). For sGAG quantification, optical densities were measured

at 595 nm. A standard curve was used to calculate total sGAG amounts in each pellet, which were then normalized on a per-DNA basis.

AFM Single-Cell Mechanical Testing. The mechanical properties of individual ASCs were measured using an atomic force microscope (MFP-3D-BIO, Asylum Research) using previously established techniques (18, 20, 21). Additional explanation of the mechanical testing procedure can be found in *SI Text*. Briefly, spherically tipped cantilevers (5 μm diameter, $k \sim 0.03$ N/m, Novascan Technologies, Inc.) were used for indentation and stress relaxation experiments. Individual cells were mechanically tested using a single indentation/stress relaxation test over the perinuclear region of the cell. An approach velocity of 15 μm/s was used, followed by a 30 s relaxation period. Cells adhered on glass substrates were tested in spherical ($n = 12$–28 cells) and spread ($n = 19$–25 cells) morphologies. Spherical cell shapes were achieved by allowing ASCs to attach for approximately 30 min. Cells within a clonal population were then tested sequentially, with the entire session lasting less than 1.5 h. After 24 h, cells spread sufficiently to exhibit flattened morphologies. Both cell shapes were confirmed visually prior to mechanical testing using phase contrast microscopy (Fig. S1). Cells attached to the glass substrate via adsorbed proteins from the culture medium, which was consistent across all clones. Specific ligand binding was not characterized in this study but could influence measured mechanical properties (51, 52). During testing, indentation depths were maximized for spherical and spread morphologies (1.2 ± 0.3 μm and 0.43 ± 0.09 μm, respectively) but never exceeded 10% strain. The elastic modulus, E_{elastic}, was extracted from force (F) vs. indentation (δ) data using a modified Hertz model [Eq. **1**] (20), where R is the relative radius of the tip, and v is the Poisson's ratio, assumed to be 0.5 for an incompressible material (53). Parametric studies showed that varying v from 0.3 to 0.5 altered the measured properties by less than 20%. The parameters E_R, E_0, and μ (relaxed modulus, instantaneous modulus, and apparent viscosity) were determined using a thin-layer, stress relaxation model of a viscoelastic solid [Eqs. **2**–**4**] (20), where τ_σ and τ_ε are the relaxation times under constant load and deformation, respectively. C is a thin-layer correction factor relating indentation depth, tip radius, and sample thickness (53). Limitations to the testing approach included a likely overestimation of elastic moduli due to a relatively fast indentation velocity (i.e., fluid pressurization contributed to the measured modulus) and an underestimation of instantaneous moduli due to an imperfect fit of the model to the initial drop during stress relaxation. However, testing procedures were identical for all cells, which allows for valid comparisons among clones in this study.

$$F(\delta) = \frac{4R^{1/2}E_{\text{elastic}}}{3(1-v^2)}\delta^{3/2}C \quad [1]$$

$$F(t) = \frac{4R^{1/2}\delta_0^{3/2}E_R}{3(1-v)}\left(1 + \frac{\tau_\sigma - \tau_\varepsilon}{\tau_\varepsilon}e^{-t/\tau_\varepsilon}\right)C \quad [2]$$

$$E_0 = E_R\left(1 + \frac{\tau_\sigma - \tau_\varepsilon}{\tau_\varepsilon}\right) \quad [3]$$

$$\mu = E_R(\tau_\sigma - \tau_\varepsilon). \quad [4]$$

Cell Sorting Simulations. A basic sorting simulation was used to assess the potential enrichment of the investigated clonal populations using lineage-appropriate mechanical biomarkers. Analysis of the mechanical properties associated with the top quartile of clones for each of the adipogenic, osteogenic, and chondrogenic lineages identified single parameters that could potentially be used for sorting (Fig. 4*A*; adipogenesis, height; osteogenesis, E_R; chondrogenesis, μ). More sophisticated approaches that take into account all measured properties are possible through clustering or neural network techniques (54). The sorting simulations involved a very basic assessment of which clonal populations would be kept if a threshold mechanical property level was set (Fig. 4 *C*–*E*). For example, keeping only clones with $E_R > 150$ Pa would result in 100% osteogenic differentiation potential in the resultant population. By moving the bar up to 200 Pa, all undiscarded clones would exhibit high osteogenic potential (Fig. 4*B*).

Statistical Analysis. Data collected from clonal populations ($n = 32$) were subjected to a Shapiro-Wilk normality test. Non-normally distributed mechanical properties were log-transformed before statistical analyses. Results for bar graphs and tables are presented as geometric mean ± SD. Differentiation potential data were normally distributed and are presented as arithmetic mean ± SD. *P*-values between differentiated and undifferentiated controls for each clone were calculated using two-tailed, unpaired student's *t*-tests ($\alpha = 0.05$). To investigate correlations between mechanical properties and differentiation potential, Pearson correlation coefficients (r) were calculated from log-transformed data. Correlation coefficients are expressed as $r \pm 95\%$ confidence intervals. Statistical significance was achieved if $P < 0.05$. All statistical tests were performed using IBM SPSS 19 software (IBM).

ACKNOWLEDGMENTS. We thank Dr. Farshid Guilak for providing resources to establish the clonal populations, as well as Poston Pritchett and Ghansham "Chris" Ramkhellawan for technical assistance and Jason Machan for advice on statistical analyses. This work was supported by National Institutes of Health (NIH) Grants from the National Institute of Arthritis and Musculoskeletal and Skin Diseases (NIAMS, AR054673) and National Institute of General Medical Sciences (NIGMS, GM104937). The contents of this publication are solely the responsibility of the authors and do not necessarily represent the official views of the NIAMS, NIGMS, or NIH.

1. Zuk PA, et al. (2001) Multilineage cells from human adipose tissue: implications for cell-based therapies. *Tissue Eng* 7:211–228.
2. Zuk PA, et al. (2002) Human adipose tissue is a source of multipotent stem cells. *Mol Biol Cell* 13:4279–4295.
3. Guilak F, et al. (2006) Clonal analysis of the differentiation potential of human adipose-derived adult stem cells. *J Cell Physiol* 206:229–237.
4. Katz AJ, Llull R, Hedrick MH, Futrell JW (1999) Emerging approaches to the tissue engineering of fat. *Clin Plast Surg* 26:587–603.
5. Aust L, et al. (2004) Yield of human adipose-derived adult stem cells from liposuction aspirates. *Cytotherapy* 6:7–14.
6. Conejero JA, et al. (2006) Repair of palatal bone defects using osteogenically differentiated fat-derived stem cells. *Plast Reconstr Surg* 117:857–863.
7. Cowan CM, et al. (2004) Adipose-derived adult stromal cells heal critical-size mouse calvarial defects. *Nat Biotechnol* 22:560–567.
8. Jeon O, et al. (2008) In vivo bone formation following transplantation of human adipose-derived stromal cells that are not differentiated osteogenically. *Tissue Eng Pt A* 14:1285–1294.
9. Yoshimura K, et al. (2010) Progenitor-enriched adipose tissue transplantation as rescue for breast implant complications. *Breast J* 16:169–175.
10. Yoshimura K, et al. (2008) Cell-assisted lipotransfer for cosmetic breast augmentation: supportive use of adipose-derived stem/stromal cells. *Aesthetic Plast Surg* 32:48–55 discussion 56–47.
11. Yoshimura K, et al. (2006) Characterization of freshly isolated and cultured cells derived from the fatty and fluid portions of liposuction aspirates. *J Cell Physiol* 208:64–76.
12. Rada T, Reis RL, Gomes ME (2011) Distinct stem cells subpopulations isolated from human adipose tissue exhibit different chondrogenic and osteogenic differentiation potential. *Stem Cell Rev* 7:64–76.
13. Gronthos S, et al. (2001) Surface protein characterization of human adipose tissue-derived stromal cells. *J Cell Physiol* 189:54–63.
14. Jones EA, et al. (2002) Isolation and characterization of bone marrow multipotential mesenchymal progenitor cells. *Arthritis Rheum* 46:3349–3360.
15. Zannettino AC, et al. (2008) Multipotential human adipose-derived stromal stem cells exhibit a perivascular phenotype in vitro and in vivo. *J Cell Physiol* 214:413–421.
16. Alt E, et al. (2011) Fibroblasts share mesenchymal phenotypes with stem cells, but lack their differentiation and colony-forming potential. *Biol Cell* 103:197–208.
17. Mitchell JB, et al. (2006) Immunophenotype of human adipose-derived cells: temporal changes in stromal-associated and stem cell-associated markers. *Stem Cells* 24:376–385.
18. Darling EM, Topel M, Zauscher S, Vail TP, Guilak F (2008) Viscoelastic properties of human mesenchymally-derived stem cells and primary osteoblasts, chondrocytes, and adipocytes. *J Biomech* 41:454–464.
19. Darling EM, et al. (2009) Mechanical properties and gene expression of chondrocytes on micropatterned substrates following dedifferentiation in monolayer. *Cellular and Molecular Bioengineering* 2:395–404.
20. Darling EM, Zauscher S, Block JA, Guilak F (2007) A thin-layer model for viscoelastic, stress-relaxation testing of cells using atomic force microscopy: do cell properties reflect metastatic potential? *Biophys J* 92:1784–1791.
21. Darling EM, Zauscher S, Guilak F (2006) Viscoelastic properties of zonal articular chondrocytes measured by atomic force microscopy. *Osteoarthritis Cartilage* 14:571–579.
22. Suresh S (2007) Biomechanics and biophysics of cancer cells. *Acta biomaterialia* 3:413–438.
23. Maloney JM, et al. (2010) Mesenchymal stem cell mechanics from the attached to the suspended state. *Biophys J* 99:2479–2487.
24. Tuan RS, Boland G, Tuli R (2003) Adult mesenchymal stem cells and cell-based tissue engineering. *Arthritis Res Ther* 5:32–45.

25. Yourek G, Hussain MA, Mao JJ (2007) Cytoskeletal changes of mesenchymal stem cells during differentiation. *ASAIO J* 53:219–228.
26. Yu H, et al. (2010) Mechanical behavior of human mesenchymal stem cells during adipogenic and osteogenic differentiation. *Biochem Biophys Res Commun* 393:150–155.
27. Titushkin I, Cho M (2007) Modulation of cellular mechanics during osteogenic differentiation of human mesenchymal stem cells. *Biophys J* 93:3693–3702.
28. Ofek G, et al. (2009) Mechanical characterization of differentiated human embryonic stem cells. *J Biomech Eng* 131:061011.
29. Lennon DP, Haynesworth SE, Arm DM, Baber MA, Caplan AI (2000) Dilution of human mesenchymal stem cells with dermal fibroblasts and the effects on in vitro and in vivo osteochondrogenesis. *Dev Dyn* 219:50–62.
30. Peptan IA, Hong L, Mao JJ (2006) Comparison of osteogenic potentials of visceral and subcutaneous adipose-derived cells of rabbits. *Plast Reconstr Surg* 117:1462–1470.
31. Estes BT, Wu AW, Storms RW, Guilak F (2006) Extended passaging, but not aldehyde dehydrogenase activity, increases the chondrogenic potential of human adipose-derived adult stem cells. *J Cell Physiol* 209:987–995.
32. Estes BT, Diekman BO, Guilak F (2008) Monolayer cell expansion conditions affect the chondrogenic potential of adipose-derived stem cells. *Biotechnol Bioeng* 99:986–995.
33. Sengenes C, Lolmede K, Zakaroff-Girard A, Busse R, Bouloumie A (2005) Preadipocytes in the human subcutaneous adipose tissue display distinct features from the adult mesenchymal and hematopoietic stem cells. *J Cell Physiol* 205:114–122.
34. Zimmerlin L, et al. (2010) Stromal vascular progenitors in adult human adipose tissue. *Cytometry A* 77:22–30.
35. Rada T, et al. (2012) Osteogenic differentiation of two distinct subpopulations of human adipose-derived stem cells: an in vitro and in vivo study. *J Tissue Eng Regen Med* 6:1–11.
36. Trickett A, Kwan YL (2003) T cell stimulation and expansion using anti-CD3/CD28 beads. *J Immunol Methods* 275:251–255.
37. Kuznetsova TG, Starodubtseva MN, Yegorenkov NI, Chizhik SA, Zhdanov RI (2007) Atomic force microscopy probing of cell elasticity. *Micron* 38:824–833.
38. Rosenbluth MJ, Lam WA, Fletcher DA (2008) Analyzing cell mechanics in hematologic diseases with microfluidic biophysical flow cytometry. *Lab Chip* 8:1062–1070.
39. Sraj I, et al. (2010) Cell deformation cytometry using diode-bar optical stretchers. *J Biomed Opt* 15:047010.
40. Sraj I, Marr DW, Eggleton CD (2010) Linear diode laser bar optical stretchers for cell deformation. *Biomedical Optics Express* 1:482–488.
41. Gossett DR, et al. (2010) Label-free cell separation and sorting in microfluidic systems. *Anal Bioanal Chem* 397:3249–3267.
42. Grover WH, et al. (2011) Measuring single-cell density. *Proc Natl Acad Sci USA* 108:10992–10996.
43. Hur SC, Henderson-MacLennan NK, McCabe ER, Di Carlo D (2011) Deformability-based cell classification and enrichment using inertial microfluidics. *Lab Chip* 11:912–920.
44. Gabriele S, Benoliel AM, Bongrand P, Theodoly O (2009) Microfluidic investigation reveals distinct roles for actin cytoskeleton and myosin II activity in capillary leukocyte trafficking. *Biophys J* 96:4308–4318.
45. Carlson RH, et al. (1997) Self-sorting of white blood cells in a lattice. *Phys Rev Lett* 79:2149–2152.
46. Lincoln B, et al. (2007) Reconfigurable microfluidic integration of a dual-beam laser trap with biomedical applications. *Biomed Microdevices* 9:703–710.
47. Lincoln B, et al. (2004) Deformability-based flow cytometry. *Cytom Part A* 59A:203–209.
48. Tan SC, et al. (2008) Viscoelastic behaviour of human mesenchymal stem cells. *BMC Cell Biol* 9:40.
49. Estes BT, Diekman BO, Gimble JM, Guilak F (2010) Isolation of adipose-derived stem cells and their induction to a chondrogenic phenotype. *Nat Protoc* 5:1294–1311.
50. Carpenter AE, et al. (2006) CellProfiler: image analysis software for identifying and quantifying cell phenotypes. *Genome Biol* 7:R100.
51. Gilchrist CL, Darling EM, Chen J, Setton LA (2011) Extracellular matrix ligand and stiffness modulate immature nucleus pulposus cell-cell interactions. *PloS one* 6:e27170.
52. Takai E, Costa KD, Shaheen A, Hung CT, Guo XE (2005) Osteoblast elastic modulus measured by atomic force microscopy is substrate dependent. *Ann Biomed Eng* 33:963–971.
53. Dimitriadis EK, Horkay F, Maresca J, Kachar B, Chadwick RS (2002) Determination of elastic moduli of thin layers of soft material using the atomic force microscope. *Biophys J* 82:2798–2810.
54. Darling EM, Guilak F (2008) A neural network model for cell classification based on single-cell biomechanical properties. *Tissue Eng Pt A* 14:1507–1515.